PHILOSOPHICAL TRANSACTIONS OF THE ROYAL SOCIETY A MATHEMATICAL, PHYSICAL & ENGINEERING SCIENCES

Simulation of the Southern Oscillation in an Atmospheric General Circulation Model

H. Von Storch, M. Latif and J. Biercamp

Phil. Trans. R. Soc. Lond. A 1989 **329**, 179-188
doi: 10.1098/rsta.1989.0069

Phil. Trans. R. Soc. Lond. A **329**, 179–188 (1989)
Printed in Great Britain

Simulation of the Southern Oscillation in an atmospheric general circulation model

By H. von Storch, M. Latif and J. Biercamp
Max-Planck-Institut für Meteorologie, Bundesstrasse 55, *D* 2000 *Hamburg* 13, *F.R.G.*

An atmospheric general circulation model (GCM) was forced with the observed near-global sea surface temperature (SST) pattern for the period January 1970–December 1985. Its response over the Pacific Ocean is compared with Tahiti and Darwin station sea-level pressure and wind stress analyses obtained from Florida State University.

The time-dependent SST clearly induces in the model run a Southern Oscillation that is apparent in the time series of all considered variables. The phase of the GCM Southern Oscillation is as observed but its low-frequency variance is too low and the spatial pattern is confined mainly to the western Pacific. The model is successful in reproducing the warm events of 1972–73 and 1982–83 and the cold event 1970–71, but fails with the cold events 1973–74 and 1975–76 and with the warm event 1976–77.

Because the GCM is used as the atmospheric component in a coupled model, the response of an equatorial oceanic primitive equation model to both the modelled and observed wind stress is examined. The ocean model responds in essentially the same way to forcing with the observed wind stress and to forcing that corresponds to the first two low-frequency empirical orthogonal functions (EOFs) of the wind variations. These first two EOFs describe a regular eastward propagation of the so signal from the western Pacific to the central Pacific within about one year. The ocean model's response to the modelled wind stress is too weak. It is similar to the response to the first observed wind stress EOF only. That is, the observed Southern Oscillation appears as a sequence of propagating patterns but the simulated Southern Oscillation appears as one standing pattern.

The nature of the deviation of simulated wind stress from observations is further analysed by means of model output statistics.

1. Introduction

In this paper we consider the ability of our atmospheric general circulation model (GCM) to reproduce observed tropical low-frequency anomalies. This model is being coupled with an oceanic GCM to study interactions between the global atmosphere and the tropical Pacific Ocean. The oceanic component is simulated with the oceanic GCM described by Latif (1987). The coupled GCM has been used to study the effect of strong westerly wind bursts in the western Pacific (Latif *et al.* 1988*a*). In another experiment, we found the coupled GCM unable to generate self-excited low-frequency variability (Latif *et al.* 1988*b*). The reasons for the model's failure were not quite clear and we speculated that the atmospheric part might be blamed for part of the failure.

Recently, a multi-year simulation was performed with the atmospheric component of the coupled GCM, by using the observed sea surface temperature (SST) for the period 1970–89. In this paper we consider the tropical response of the atmospheric model to these SST anomalies, which include several cold and warm events.

2. Data

The atmospheric model was developed at the European Centre for Medium Range Weather Forecasting (the T21 model) and is described by Fischer (1987) and von Storch (1988). It was run over 16 years by using observed SST (Reynolds 1988); (40° S–60° N from 1970 to 1980; global from 1981 to 1985). Over land, temperature and moisture have been calculated prognostically by using prescribed deep-soil temperature and moisture. The distribution and surface temperature of sea and land ice have been prescribed. The initial conditions are taken from 1 January, year 2, of a control run with climatological SST. The model output is stored as monthly means, which are indexed by the date of the SST anomaly.

As verification data we use the sea-level pressure difference between Darwin and Tahiti and time series of monthly mean pseudo-stress fields, which have been obtained from subjective analyses of ship observations over the tropical Pacific. This Florida State University (FSU) wind data set (Goldenberg & O'Brien 1981; Legler & O'Brien 1984) has a resolution of 2° × 2°. The analysed area extends from 29° N to 29° S and from 124° E to 70° W. Data are available for the period 1961–1985.

3. Comparison: simulated data against observations

As a measure of the state of the Southern Oscillation we use the monthly mean sea-level pressure (SLP) difference between Darwin and Tahiti. The observed and simulated time series are shown in figure 1. The two time series are not related to each other on timescales of a few months, but on timescales longer than a year the signs of the simulated and the observed Southern Oscillation indices (SOIS) coincide. Also, the observed warm events 1972–73 and 1982–83 are nicely reproduced by the model, and so is the cold phase of 1970–71. On the other hand, the model fails to reproduce the pair of cold events 1973–74 and 1975–76 and the period of fairly high SOI during 1976–77.

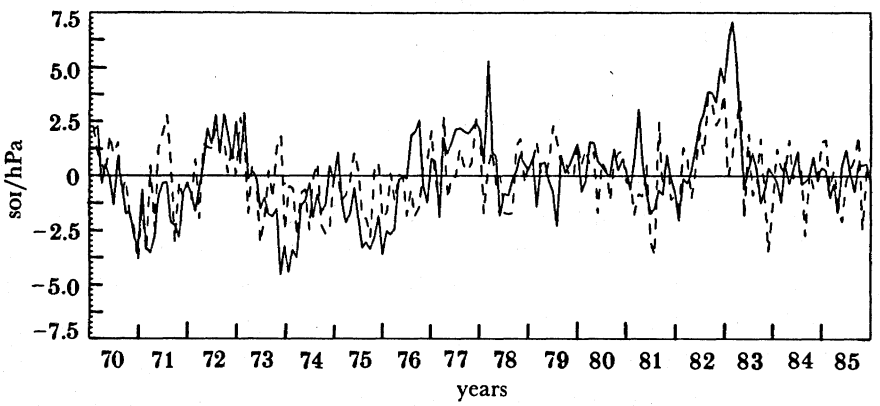

Figure 1. Simulated (broken line) and observed (solid line) Southern Oscillation index (SOI) defined by the monthly mean difference of sea-level pressure anomalies at Darwin and Tahiti.

The statistics of the two curves is summarized in the auto, coherence squared and phase spectra, shown in figure 2. On timescales shorter than one year, the variances of both time series are similar, but the coherence is low. On timescales longer than two years, the GCM-generated variance is clearly weaker than the observed variance. The coherence, however, is large (80% and more) and highly significant (risk less than 1%) at these timescales and the phase spectrum

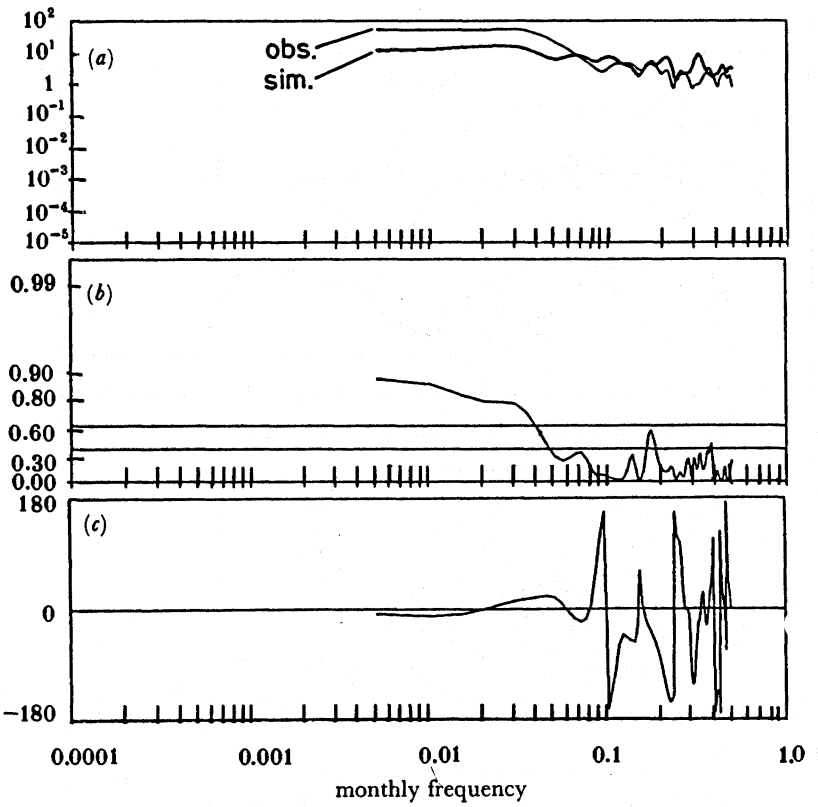

FIGURE 2. Auto (*a*), coherence squared (*b*) and phase (*c*) spectra of the simulated (heavy line) and observed (light line) Southern Oscillation index shown in figure 1.

is close to zero. We conclude that the timing of the simulated low-frequency Southern Oscillation is adequately reproduced, but that the intensity of modelled SOI is too weak.

Empirical orthogonal function (EOF) analyses of low pass filtered (periods of less than 16 months have been removed) wind stress anomalies have been carried out for the Florida State University data set and for the GCM results. In both cases the first two EOFs, E_1 and E_2, of anomalous zonal wind stress contribute more than half of its total variance (observation: 34 % and 19 %; simulation: 42 % and 18 %) whereas subsequent EOFs each contribute less than one tenth.

Both first (second) EOFs as well as their principal components are shown in figure 3 (4). The spatial characteristics of E_1^{obs} and E_1^{GCM} are quite similar with large positive values over the western tropical Pacific with maximum on the equator at the dateline and smaller negative values east of 130° W. The tongue of positive values extending from the maximum to the southeast, reminiscent of the South Pacific convergence zone (SPCZ), which is seen in the observations, is not present in the simulations. The pattern of E_2^{obs} and E_2^{GCM} also show some similarities. In both patterns we find positive values on the Equator except for its westernmost part, positive maxima at about 150° W, 10° S and negative maxima north of Australia.

The corresponding principal components (*PC*) are shown in figures 3*c* and 4*c*. In the observed time series, PC_1^{obs}, all warm and cold events are easily identified, but in the simulated time series, PC_2^{GCM} only the strong events of 1972–73 and 1982–83, as well as the moderate cold phase before 1972, are captured. Cross-spectral analysis (not shown) reveals that the two curves have significant coherence squared for periods longer than 20 months.

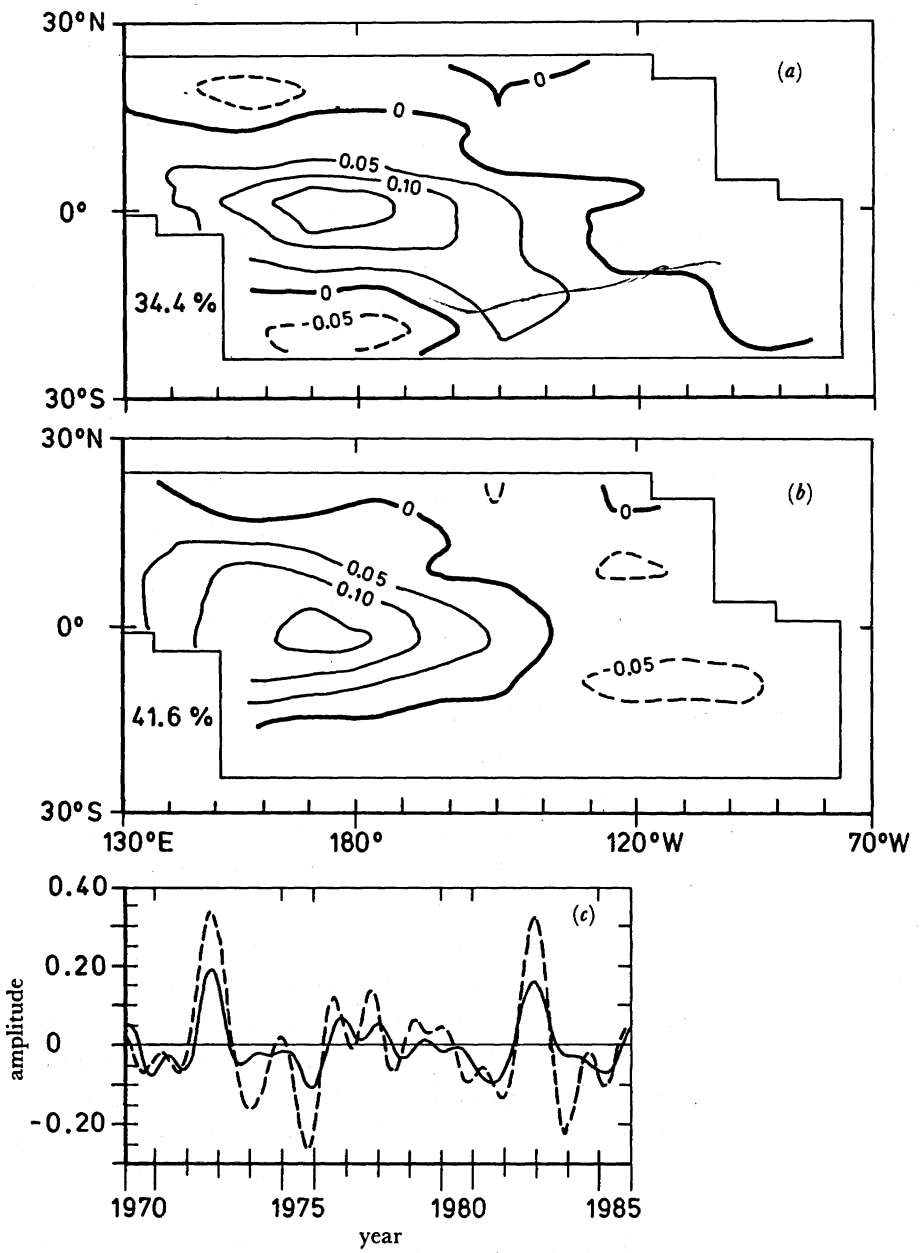

FIGURE 3. First empirical orthogonal functions (EOFs) of zonal wind stress derived from 1970–85 Florida State University analyses (*a*) and from the GCM experiment (*b*). The explained variance is 34.4 % for the observation and 41.6 % for the simulation. The corresponding coefficients are shown in (*c*). Broken line: FSU analyses. Solid line: GCM experiment.

Whereas E_1^{obs} and E_1^{GCM} describe the development and distribution of anomalies at the 'centre of action' of the Southern Oscillation, i.e. the occurrence of wind anomalies west of the dateline, E_2^{obs} (shown in figure 4*a*), seems to describe the migration of these anomalies across the Pacific basin. As can be seen from figure 4*c*, the coefficient time series PC_1^{obs} and PC_2^{obs} of the first and second observed EOFs vary over most of the 16 year period quite coherently with a phase shift of one half to one year. This may be interpreted as a 'rotational mode' with E_1^{obs} (figure 3*a*) showing the distribution of anomalies at the time of El Niño (or La Niña) events

PHILOSOPHICAL TRANSACTIONS OF THE ROYAL SOCIETY A MATHEMATICAL, PHYSICAL & ENGINEERING SCIENCES

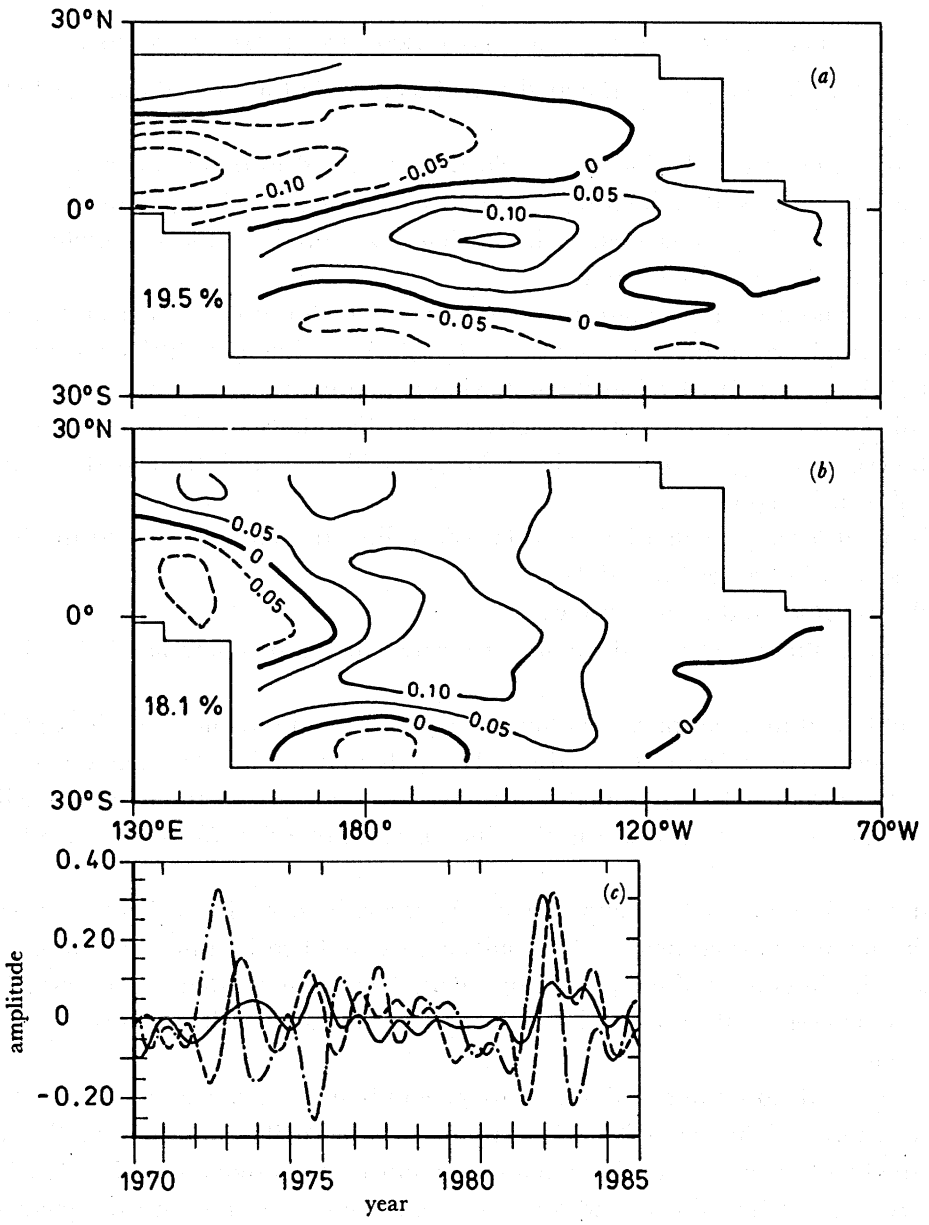

FIGURE 4. As figure 3 but for second EOFs and explained variance 19.5% (observation) and 18.1% (simulation). In (*c*), solid line, simulation; dot-dash line, observation 1; broken line, observation 2.

and E_2^{obs} (figure 4*a*) describing an eastward shift during the transition phases between these events.

From the GCM-simulated stress field, no EOF could be found that plays the role of the second observation. For instance, the coefficient time series PC_2^{GCM} of the second simulated EOF E_2^{GCM} (solid line in figure 4*c*) hardly shows any resemblance to the observed time series PC_2^{obs}.

4. Sensitivity of the ocean to wind stress differences

The findings of the EOF analysis of simulated and observed wind stress lead us to the following two hypotheses.

(i) That part of the observed wind stress field that is related to the occurrence of El Niño and La Niña events may be described by the first two EOFs E_1^{obs} and E_1^{GCM} only.

(ii) The simulated wind stress field is insufficient to reproduce the complete observed sequence of El Niño and La Niña events.

To assess these hypotheses the equatorial oceanic GCM, which is used in the coupled tropical ocean global atmosphere (TOGA) GCM (Latif *et al.* 1988*a*, *b*), has been driven with various forcing fields of the period 1970–85 in the following experiments.

(A) The full *observed* wind stress forcing derived from Florida State University analyses;

(B) the observed forcing, which has been low-pass filtered and truncated to the first observed EOF shown in figure 3*a*;

(C) the observed forcing, which has been low-pass filtered and truncated to the first two observed EOFs shown in figures 3*a* and 4*a*;

(D) the full *simulated* wind stress forcing;

(E) the low-pass filtered simulated forcing truncated to the first simulated EOF shown in figure 3*b*.

The results obtained in experiment (A) have been presented in detail by Latif (1987), who compared the simulated SST with observed SST. He finds that the low-frequency variation of SST is favourably reproduced by the model in the western Pacific. In the eastern Pacific the results are less satisfying, but at least the El Niño episodes of 1972–73 and 1982–83 can be identified.

In this section we use the results of experiment (A) as a reference with which to compare the SST obtained in the other experiments. The results are exemplified by time series of simulated SST anomalies at the dateline on the Equator (figure 5). The SSTs simulated in (D) and (E) were almost identical. Therefore, the SST simulated in (E) is not shown. Similar results are obtained at other locations.

Experiment (B) leads to SST anomalies that are generally much weaker than those obtained in the reference run (A). This is particularly so in the eastern Pacific (not shown). The forcing truncated to the first EOF excites, at the dateline, the full El Niño signal only in 1972–73 and 1982–83 (figure 5*a*). Adding the second EOF, i.e. experiment (C), dramatically changes the simulated SST, which becomes quite similar to the SST of the reference run. We conclude that the ocean GCM experiments strongly support our hypothesis (i).

The SST obtained when the ocean is forced with GCM simulated wind stress (experiment (D)) is shown in figure 5*b*. As might have been suspected from wind stress itself, the variance of SST is considerably reduced. The El Niño Southern Oscillation (ENSO) signal in the western Pacific is, again apart from the two warm events of 1972–73 and 1982–83 much too weak. Thus, hypothesis (ii) turns out to be correct also.

More important than the general underestimation of the SST, however, is the similarity of the experiment (D) curves with those obtained in the experiments (B) and (E), when only the first observed or simulated EOFs were used. From this similarity we infer that there is nothing in the simulated wind field that could play the rôle of the second observed EOF, and that the so-related signal in the simulations may readily be represented by the first simulated EOF only. We

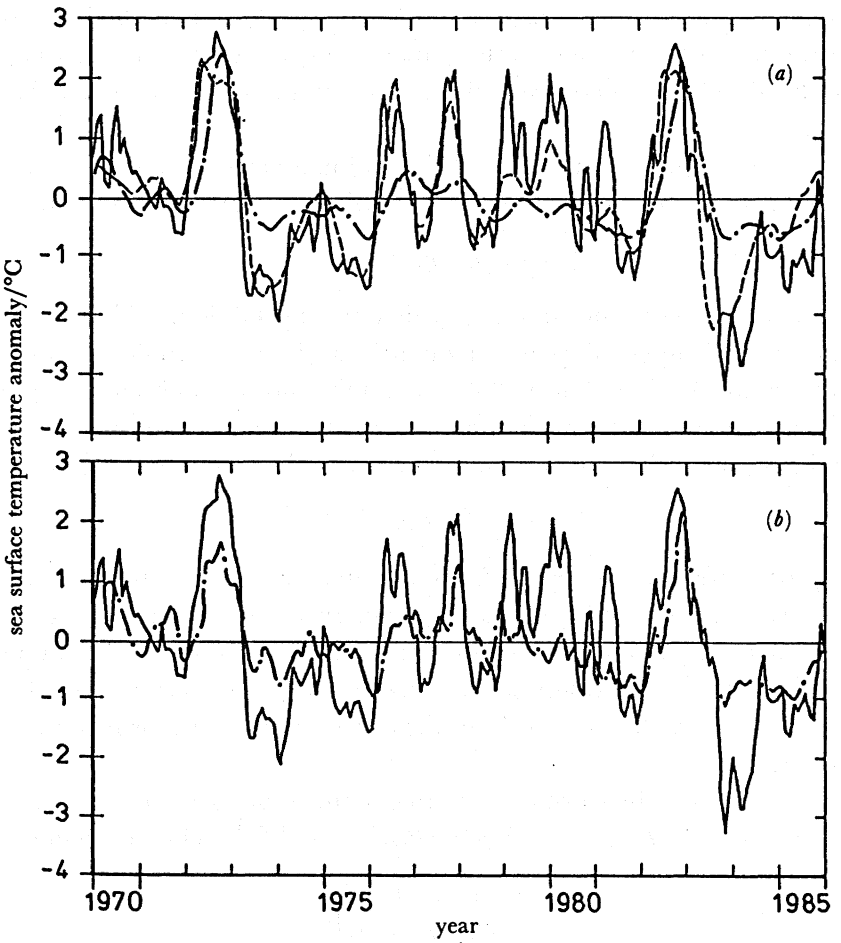

FIGURE 5. SST response of the ocean GCM on the Equator at the dateline to (*a*) observed and (*b*) simulated wind stress. The solid line show the SST anomalies which are obtained in the reference experiment (A) when the ocean model is forced with the Florida State University analyses. (*a*) Dash–dot line, response to forcing which has been truncated to first observed EOF (experiment (B)); broken line, response to forcing truncated to the first two EOFs, i.e. experiment (C). (*b*) Dash–dot line, response to full GCM simulated wind stress field (experiment (D)). When truncated to the first simulated EOF (experiment E), the SST anomaly is nearly unchanged.

conclude that the real Southern Oscillation may be identified with the stochastic cyclic sequence of patterns,

$$\ldots \to E_1^{\mathrm{obs}} \to E_2^{\mathrm{obs}} \to -E_1^{\mathrm{obs}} \to -E_2^{\mathrm{obs}} \to E_1^{\mathrm{obs}} \to E_2^{\mathrm{obs}} \ldots .$$

This sequence describes a smooth eastward propagation. The model's sequence, however, appears as a mainly standing pattern variation:

$$\ldots \to E_1^{\mathrm{GCM}} \to -E_1^{\mathrm{GCM}} \to E_1^{\mathrm{GCM}} \to -E_1^{\mathrm{GCM}} \to \ldots .$$

5. STATISTICAL *A POSTERIORI* IMPROVEMENT OF SIMULATED WIND STRESS

The results of the atmospheric GCM response found in the previous section are disappointing because they indicate that the atmospheric GCM in its present form is not well suited as the atmospheric part of a coupled TOGA model. A possibility for overcoming the shortcomings in simulated wind stress, at least for ENSO prediction studies with our coupled system, may be the

application of model output statistics (MOS) (Glahn & Lowry 1972), a method that is routinely used in operational weather forecasting. In this paper we use the technique as a diagnostic tool to find out how the simulated wind stress fields may be improved to give a better ocean response.

If the observations are represented by an $\mathscr{M}$-dimensional vector $\boldsymbol{q}$ and the simulated data by an $\mathscr{N}$-dimensional vector $\boldsymbol{p}$, we are looking for a $\mathscr{M}\times\mathscr{N}$ matrix $\mathscr{L}$ minimizing

$$\langle\|\mathscr{L}\boldsymbol{p}_t-\boldsymbol{q}_t\|^2\rangle, \tag{1}$$

where $\|\cdot\|$ is the euclidean vector norm and $\langle\cdot\rangle$ denotes expectation. $\mathscr{L}$ is a linear operator that tells us what the $\mathscr{M}$ observed physical quantities q^1 to $q^{\mathscr{M}}$ would be on average, if the model simulates p^1 to $p^{\mathscr{N}}$. Note that neither the number nor the parameter represented by the vectors $\boldsymbol{q}$ and $\boldsymbol{p}$ have to be the same. For instance, $\boldsymbol{q}$ might represent 850 mbar† zonal wind on a fine grid and $\boldsymbol{p}$ surface wind stress on a coarse grid. The solution of (1) is given by

$$\mathscr{L}=\langle\boldsymbol{q}_t\boldsymbol{p}_t^{\mathrm{T}}\rangle\cdot\langle\boldsymbol{p}_t\boldsymbol{p}_t^{\mathrm{T}}\rangle^{-1}. \tag{2}$$

After determining the 'correction matrix' $\mathscr{L}$, the GCM-generated wind stress can be corrected interactively in the coupled atmosphere–ocean system. In the present paper we consider the possible merits of doing so by forcing the ocean GCM with *a posteriori* corrected wind stress, i.e., by $\mathscr{L}\boldsymbol{p}$ instead of by $\boldsymbol{p}$ alone. The result of the correction is a time series of zonal wind stress anomalies, whose statistics are determined from the observations, whereas its time evolution is computed by the GCM.

For $\boldsymbol{p}$ and $\boldsymbol{q}$, we use the two first principal components of low pass filtered wind stress, i.e. $\mathscr{N}=\mathscr{M}=2$ and $\boldsymbol{q}=(PC_1^{\mathrm{obs}},PC_2^{\mathrm{obs}})^{\mathrm{T}}$ and $\boldsymbol{p}=(PC_1^{\mathrm{GCM}},PC_2^{\mathrm{GCM}})^{\mathrm{T}}$. The correction matrix $\mathscr{L}$ derived from (2) is

$$\mathscr{L}=\begin{pmatrix}1.71 & 0.53\\ -0.23 & 1.40\end{pmatrix}.$$

This matrix describes an enhancement of the simulated principal components (the main diagonal elements are larger than 1) and a slight mixture of the two EOF coefficients.

The *a posteriori* correction of the wind stress used to force the ocean GCM is given by

$$\tau^*=\tau-[(E_1^{\mathrm{obs}},E_2^{\mathrm{obs}})\cdot\mathscr{L}-(E_1^{\mathrm{GCM}},E_2^{\mathrm{GCM}})]\begin{pmatrix}PC_1^{\mathrm{GCM}}\\ PC_2^{\mathrm{GCM}}\end{pmatrix},$$

where τ denotes the 'raw' GCM-simulated wind stress and τ^* the corrected stress. Note that the MOS approach not only changes the variance but also the patterns by replacing the simulated EOF patterns with the observed EOF patterns.

The results of the MOS approach are presented by showing the ocean GCMs response to the MOS corrected GCM wind stress at the equatorial location already used in §4, namely 180° (figure 6). On the ENSO timescale MOS leads to a dramatic improvement: the reference curve and the MOS curve are almost identical. Exceptions are the strong cooling following the 1982–83 event and the large positive anomalies during 1979 and 1980 in the western Pacific. Interestingly, neither of these features are found in observations (see the Southern Oscillation index, figure 1). So one might speculate (but by no means be certain), that by combining the information from both Florida State University analyses and GCM output, and by restricting ourselves to the dominant

† 1 mbar = 10^2 Pa.

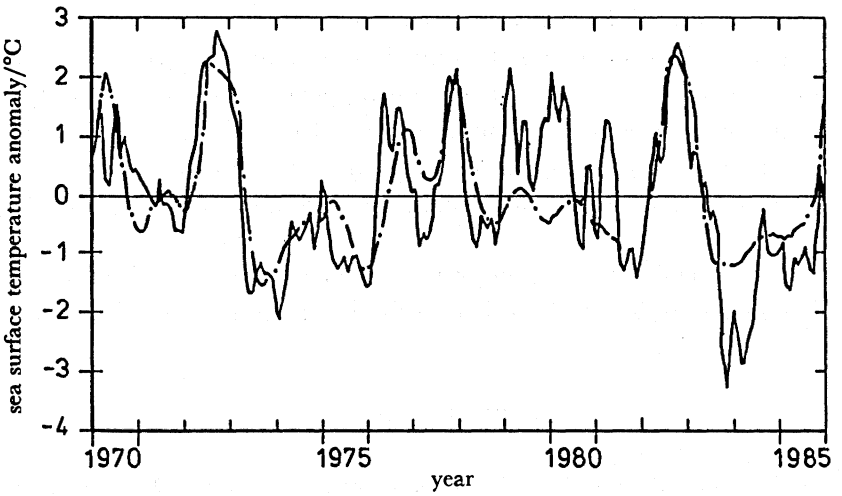

FIGURE 6. SST response of the ocean GCM on the Equator at the dateline to the MOS-corrected simulated wind stress. The solid line shows the SST anomalies, which are obtained in the reference experiment (A) when the ocean model is forced with the Florida State University analyses. Broken line, response to MOS-corrected wind stress.

parts, we can improve the forcing fields in some aspects. At other equatorial locations, e.g. in the eastern equatorial Pacific, MOS leads to a moderate improvement.

Use of more than two EOF coefficients in equation (1) did not improve our results significantly. That, however, it is not sufficient to use only the first EOF can be deduced from hypothesis (i) presented in the preceding section.

6. Discussion

There are two main conclusions to be drawn.

1. The Southern Oscillation has phase propagation that may be described as the sum of two patterns. This conclusion is in accord with findings by Barnett (1985), van Loon & Shea (1985, 1987) and Xu & von Storch (1989) who identified with various techniques (complex EOFs, composites, principal oscillation patterns) cyclic sequences

$$\ldots \rightarrow P \rightarrow Q \rightarrow -P \rightarrow -Q \rightarrow P \rightarrow \ldots,$$

which may be exploited for predictive purposes (Barnett *et al.* 1988; Xu & von Storch 1989).

2. Sea surface temperature variations induce a Southern Oscillation in the atmospheric GCM. It is a standing pattern oscillation, and has too little energy in the Southern Oscillation frequency band. The modelled and the simulated Southern Oscillation indices are highly coherent on the interannual timescale. A GCM experiment similar to ours has been done at the Geophysical Fluid Dynamics Laboratory (GFDL). Lau (1985) performed a 15 year integration using observed month-to-month SSTs during the period 1962–76 as lower-boundary condition over the tropical Pacific. He and Barnett (1985) show that the model's circulation in the tropics responds to SST changes during El Niño events with a model Southern Oscillation index, which is realistic in phase but too weak compared with reality. Also in this experiment, the Southern Oscillation appears as mainly standing in contrast to the real Southern Oscillation that is a propagating feature.

A minor conclusion refers to the MOS (model output statistics) technique that we have used

to diagnose the model's tropical Pacific wind stress field. In the *a posteriori* mode we could linearly transform the modelled wind stress to a much more realistic time series. The potential success of MOS is, however, limited because of the missing pendant of the second observed wind stress EOF. First tests of the interactive use of MOS in the coupled model are not very encouraging. As an alternative to the pattern-oriented MOS approach used in this paper one could use LOS (local output statistics), which is the application of the MOS estimate separately at each grid point.

We thank Marion Grunert for thoroughly preparing the diagrams, Dr Edilbert Kirk for the GCM data, Peter Wright for the SOI and Dr J. J. O'Brien for the pseudo-wind stress data.

References

Barnett, T. P. 1985 *J. atmos Sci.* **42**, 478–501.
Barnett, T. P., Graham, N., Cane, M., Zebiak, S., Dolan, S., O'Brien, J. & Legler, D. 1988 *Science Wash.* **241**, 192–196.
Fischer, G. (ed.) 1987 *Large scale atmospheric modelling report no.* 1, Meteorologisches Institut der Universität Hamburg.
Glahn, H. R. & Lowry, D. A. 1972 *J. appl. Meteor.* **11**, 1203–1211.
Goldenberg, S. B. & O'Brien, J. J. 1981 *Mon. Wea. Rev.* **109**, 1190–1207.
Latif, M. 1987 *J. phys. Oceanogr.* **17**, 246–263.
Latif, M., Biercamp, J. & von Storch, H. 1988*a* *J. atmos. Sci.* **45**, 964–979.
Latif, M., Biercamp, J., von Storch, H. & Zwiers, F. W. 1988*b* Max-Planck-Institut für Meteorologie, report no. 17.
Lau, N.-C. 1985 *Mon. Wea. Rev.* **113**, 1970–1996.
Legler, D. M. & O'Brien, J. J. 1984 *Atlas of tropical Pacific wind stress climatology 1971–1980.* Florida State University, Department of Meteorology.
Reynolds, R. W. 1988 *J. Climate* **1**, 75–86.
von Storch, H. (ed.) 1988 *Large scale atmospheric modelling report no.* 4, Meteorologisches Institut der Universität Hamburg.
van Loon, H. & Shea, D. J. 1985 *Mon. Wea. Rev.* **113**, 2063–2074.
van Loon, H. & Shea, D. J. 1987 *Mon. Wea. Rev.* **115**, 370–379.
Xu, J.-S. & von Storch, H. 1989 Prediction of the SO by POP analysis. Max-Planck-Institut für Meteorologie Report. (In the press.)

PHILOSOPHICAL TRANSACTIONS OF THE ROYAL SOCIETY A MATHEMATICAL, PHYSICAL & ENGINEERING SCIENCES